

## Material Removal Model Considering Influence of Curvature Radius in Bonnet Polishing Convex Surface

SONG Jianfeng<sup>1,2,\*</sup> and YAO Yingxue<sup>2</sup>

<sup>1</sup> College of Mechanical Engineering, Yanshan University, Qinhuangdao 066004, China

<sup>2</sup> Digital Manufacturing Laboratory of Mechatronics Engineering College, Harbin Institute of Technology, Harbin 150001, China

Received May 28, 2014; revised March 23, 2015; accepted September 23, 2015

**Abstract:** The bonnet tool polishing is a novel, advanced and ultra-precise polishing process, by which the freeform surface can be polished. However, during the past few years, not only the key technology of calculating the dwell time and controlling the surface form in the bonnet polishing has been little reported so far, but also little attention has been paid to research the material removal function of the convex surface based on the geometry model considering the influence of the curvature radius. Firstly in this paper, for realizing the control of the freeform surface automatically by the bonnet polishing, on the basis of the simplified geometric model of convex surface, the calculation expression of the polishing contact spot on the convex surface considering the influence of the curvature radius is deduced, and the calculation model of the pressure distribution considering the influence of the curvature radius on the convex surface is derived by the coordinate transformation. Then the velocity distribution model is built in the bonnet polishing the convex surface. On the basis of the above research and the semi-experimental modified Preston equation obtained from the combination method of experimental and theoretical derivation, the material removal model of the convex surface considering the influence of the curvature radius in the bonnet polishing is established. Finally, the validity of the model through the simulation method has been validated. This research presents an effective prediction model and the calculation method of material removal for convex surface in bonnet polishing and prepares for the bonnet polishing the free surface numerically and automatically.

**Keywords:** bonnet polishing, convex surface, material removal model, curvature radius

### 1 Introduction

The bonnet tool polishing was a novel ultra precise polishing method and can be used for machining freeform surfaces with high accuracy and good surface roughness<sup>[1-2]</sup>. The Zeeko Ltd and University College London in the United Kingdom jointly researched the bonnet polishing machines IRP200 in 2000<sup>[3-4]</sup>, which can make the surface roughness up to 3 nm ( $R_a$ ) by the precession polishing<sup>[5]</sup>. In subsequent research, the surface shape accuracy can be made up to 80 nm (P-V) for aspheric parts<sup>[6]</sup>. JACOBS<sup>[7]</sup> from University of Rochester in United States in 2004 presented the viewpoint that the bonnet polishing was one of six international innovations in optical finishing. All above papers show that the bonnet polishing is an effective ultra precision polishing method.

In addition, KIM, et al<sup>[8-9]</sup>, in Korea researched the Algorithm simulation on the surface control by the bonnet polishing technology. BEAUCAMP, et al<sup>[10]</sup>, in Japan not

only used the computer numerical control precession bonnet polishing technology to the corrective finishing of photomask substrates for EUV lithography but also polished the tungsten carbide moulds including any aspheric and freeform shape by 7-axis CNC precession polishing machine and demonstrated the ability of correcting surface form in bonnet polishing<sup>[11]</sup>. However, the key technology for realizing the free surface automatic control in the bonnet polishing such as the technology of calculating dwell time and controlling surface form has not been reported so far.

In China, the research of the bonnet polishing technology has just been started. At present, PAN, et al<sup>[12-13]</sup>, in Xiamen University built the bonnet polishing experimental platform and studied the precession control technology for large diameter aspheric; WANG, et al<sup>[14]</sup>, in Xiamen University not only presented one self-adaptive iterative algorithm to calculate the dwell time when polishing large optics but also investigated three kinds models of static tool influence function (sTIF) based FEA<sup>[15]</sup>, and WANG, et al<sup>[16]</sup>, further investigated the optimization parameters for bonnet polishing based on the minimum residual error method. The team of Professor JI in Zhejiang University of Technology has researched the mould technology for

\* Corresponding author. E-mail: songjianfeng@ysu.edu.cn

Supported by Young Teacher Independent Research Subject of Yanshan University of China (Grant No. 15LGA002)

© Chinese Mechanical Engineering Society and Springer-Verlag Berlin Heidelberg 2015

freeform surface using the bonnet polishing till now<sup>[17-21]</sup>. Harbin Institute Technology built the experimental prototype machine in 2004 and had started to engage the development of the bonnet polishing parallel machine and to develop CNC system of the parallel machine in recent years<sup>[22-23]</sup>.

However, little attention has been paid to research the material removal function based on the geometry model for curved workpieces considering the influence of the curvature radius. For realizing the freeform surface automatic control, the above-mentioned research was developed in this paper.

Firstly, in this paper, for the convex surface, the pressure distribution regular expression and the relative velocity distribution regular expression that are related to the curvature radius of the curved workpiece has been deduced, then the semi-experimental material removal model considering the curvature radius of the workpiece has been built, finally the validity of the model through the experimental method and the simulation method has been validated.

## 2 Pressure Distribution Considering Influence of Curvature Radius in Bonnet Polishing Convex Surface

Most of the earlier models were at the macro-scale, and were based on the Preston's law<sup>[24]</sup>, the integrate Material Removal Rate can be expressed by the following equation:

$$\frac{dh}{dt} = K_p P V, \quad (1)$$

where  $dh/dt$  is the material removal rate,  $P$  is the applied pressure,  $V$  is the relative velocity between the workpiece and the polishing tool,  $K_p$  is Preston coefficient.

In the bonnet polishing, the bonnet is in compression, the polishing spot will be generated. Hence the polishing pressure on the polishing spot mainly originates from the bonnet decrement; the polishing tool itself rotational speed is more quickly than that of the workpiece, the relative velocity between the polishing tool and the workpiece mainly originates from the bonnet rotational speed. So the bonnet decrement and the relative velocity are two main ingredients influencing on the material removal rate.

In addition, the workpiece surface which can be polished by the bonnet polishing are diversiform, includes: the flat surface, the convex surface, the concave surface, even aspheric surface and freeform surface. So the curvature radius of the workpiece is the additional ingredient influencing on the material removal rate. As the material removal model is investigated, the curvature radius of the curved workpiece need to be taken into account.

### 2.1 Theoretical expression derivation of pressure distribution

The pressure applied in the contact region is caused by

the elastic deformation of the bonnet itself and the initial inner pressure of the puffed bonnet. The puffed bonnet can be considered as the linear elastic system and can be expressed by the spring model. Under the different pressure, the elastic coefficient of the bonnet  $k$  is different. The bonnet inner pressure increases with the increasing of the external pressure<sup>[23]</sup>. With the inner pressure increasing, the elastic coefficient  $k$  increases, it can lead to the increasing of the load on the contact region.

So, the force  $F$  exerted on the workpiece can be calculated as

$$F = KH, \quad (2)$$

where  $K$  is the coefficient of elasticity (N/mm);  $H$  is the bonnet decrement of the arbitrary point in the polishing contact area (mm).

According to Hertz contact theory<sup>[25]</sup>, the average pressure in contact area can be expressed by

$$P = \frac{F}{\pi ab}, \quad (3)$$

where  $a$  is the length of major semi-axis in the elliptical contact zone (mm);  $b$  is the length of minor semi-axis in the elliptical contact zone (mm).

The bonnet and the workpiece are all sphere and space axial symmetric geometry. The geometric model of the bonnet polishing convex spherical workpiece can be simplified as Fig. 1.

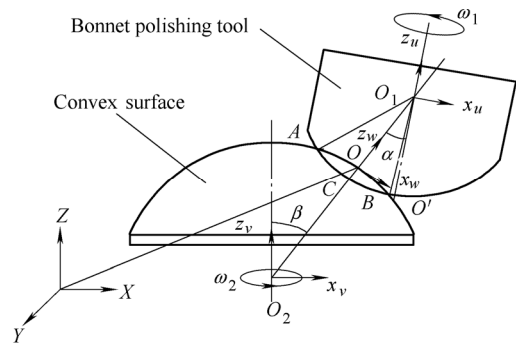


Fig. 1. Geometric model of the bonnet polishing the convex surface

As shown in Fig. 1, the point  $O_1$  is the spherical center of the bonnet,  $O_2$  is the spherical center of the workpiece,  $O$  is the center of the polishing contact region,  $O'$  is the zero point of line speed on the external surface of the bonnet,  $\alpha$  is the included angle between the rotation axis of the bonnet and the normal of the center point on the contact region (precession angle),  $\beta$  is the included angle between the rotation axis of the workpiece and the normal line of the center point on the contact region. In Fig. 1, supposing  $XYZ$  is the integral coordinate system in the geometrical model, and  $x_u y_u z_u$ ,  $x_v y_v z_v$  and  $x_w y_w z_w$  are the local coordinate system. Among these coordinate system, the original point of  $x_u y_u z_u$

coordinate is located the sphere center point  $O_1$  of the bonnet, the original point of  $x_v, y_v, z_v$  coordinate is located the sphere center point  $O_2$  of the workpiece, the original point of  $x_w, y_w, z_w$  coordinate is located the center  $O$  of the contact region with the ellipse shape. The meaning of symbols in Fig. 1 is shown in Table 1.

**Table 1. Symbol meaning**

Symbol	Meaning
$X, Y, Z$	Integral coordinate system
$x_w, y_w, z_w$	Local coordinate system in the symmetrical center point on the oval-shaped contact region
$x_u, y_u, z_u$	Local coordinate system in the bonnet center
$x_v, y_v, z_v$	Local coordinate system in the workpiece center
$R_1$	Curvature radius of the bonnet
$R_2$	Curvature radius of the workpiece
$\omega_1$	Rotational speed of the bonnet
$\omega_2$	Rotational speed of the workpiece
$a$	Semi-major axis dimension of oval-shaped polishing spot
$b$	Semi-minor axis dimension of oval-shaped polishing spot
$h$	Bonnet decrement
$\alpha$	Precession angle
$\beta$	Included angle between the rotation axis of the workpiece and the normal of the center point on the contact region
$OC$	Decrement in the initial contact point $O$ between the bonnet and the convex sphere
$\widehat{AOB}$	Length of the contact arc line after the convex sphere workpiece and the bonnet are in compression
$ AB $	Distance of $AB$ (the diameter length of the contact region between the convex sphere and the bonnet)

As the workpiece is static ( $\omega_2 = 0$ ), the pressure distribution expression can be deduced in the bonnet polishing.

Firstly during the coordinate system  $x_u, y_u, z_u$  and the coordinate system  $x_w, y_w, z_w$ , the coordinate transformation will be implemented, Eqs. (4) and (5) will be obtained:

$$\begin{cases} x_u = x_w \cos(-\alpha) - [z_w - (R_1 - h)] \sin(-\alpha), \\ y_u = y_w, \\ z_u = x_w \sin(-\alpha) + [z_w - (R_1 - h)] \cos(-\alpha), \end{cases} \quad (4)$$

$$x_u^2 + y_u^2 + z_u^2 = R_1^2. \quad (5)$$

Substituting Eq. (4) into Eq. (5), and Eq. (6) can be obtained:

$$x_w^2 + y_w^2 + z_w^2 + (R_1 - h)^2 - 2z_w(R_1 - h) = R_1^2. \quad (6)$$

For the local coordinate system  $x_v, y_v, z_v$  and  $x_w, y_w, z_w$ :

$$\begin{cases} x_v = x_w \cos(-\beta) - (z_w + R_2) \sin(-\beta), \\ y_v = y_w, \\ z_v = x_w \sin(-\beta) + (z_w + R_2) \cos(-\beta), \end{cases} \quad (7)$$

$$x_v^2 + y_v^2 + z_v^2 = R_2^2. \quad (8)$$

Substituting Eq. (7) into Eq. (8), and Eq. (9) can be

obtained after simplifying:

$$x_w^2 + y_w^2 + z_w^2 + 2z_w R_2 = 0. \quad (9)$$

The simplified simultaneous Eq. (10) from Eqs. (6) and (9) can be expressed as follows:

$$\begin{cases} x_w^2 + y_w^2 + z_w^2 + (R_1 - h)^2 - 2z_w(R_1 - h) = R_1^2, \\ x_w^2 + y_w^2 + z_w^2 + 2z_w R_2 = 0. \end{cases} \quad (10)$$

The solution is

$$z_w = \frac{h^2 - 2R_1 h}{2(R_1 + R_2 - h)}. \quad (11)$$

Substituting Eq. (11) for Eq. (10):

$$\begin{cases} x_w^2 + y_w^2 = [h(2R_1 - h)(h^2 - 2R_1 h - 4R_2 h + 4R_1 R_2 + 4R_2^2)] / 4(R_1 - h + R_2)^2, \\ z_w = \frac{h^2 - 2R_1 h}{2(R_1 + R_2 - h)}. \end{cases} \quad (12)$$

According to Eq. (12), the polishing contact spot can be regarded as the round between the spherical bonnet and the workpiece.

Eq. (6) is solved to obtain the two value of  $z_w$ , respectively the symbol  $z_{w11}$  and the symbol  $z_{w12}$  will be shown:

$$\begin{cases} z_{w11} = R_1 - h + \sqrt{R_1^2 - x_w^2 - y_w^2}, \\ z_{w12} = R_1 - h - \sqrt{R_1^2 - x_w^2 - y_w^2}. \end{cases} \quad (13)$$

Eq. (9) is solved, and the solution can be used the symbol  $z_{w21}$  and the symbol  $z_{w22}$  to show respectively:

$$\begin{cases} z_{w21} = -R_2 + \sqrt{R_2^2 - x_w^2 - y_w^2} \\ z_{w22} = -R_2 - \sqrt{R_2^2 - x_w^2 - y_w^2} \end{cases} \quad (14)$$

According to the coordinate direction of the local coordinate system  $x_w, y_w, z_w$ , the solution  $z_w$  is

$$\begin{aligned} z_{w1} = z_{w12} &= R_1 - h - \sqrt{R_1^2 - x_w^2 - y_w^2}; \\ z_{w2} = z_{w21} &= -R_2 + \sqrt{R_2^2 - x_w^2 - y_w^2}. \end{aligned}$$

Because

$$H = \int_{z_{w2}}^{z_{w1}} dy = z_{w1} - z_{w2}. \quad (15)$$

According to Eq. (2), the pressure applied by the bonnet can be expressed by the following expression:

$$F = kH = k \int_{z_{w2}}^{z_{w1}} dy = k(z_{w1} - z_{w2}). \quad (16)$$

Then

$$H = \int_{z_{w2}}^{z_{w1}} dz = -h + (R_1 - \sqrt{R_1^2 - x_w^2 - y_w^2}) + (R_2 - \sqrt{R_2^2 - x_w^2 - y_w^2}). \quad (17)$$

According to Eqs. (16) and (17), when polishing the convex surface, the pressure of the arbitrary point on the polishing spot can be expressed as the following expression:

$$F_t(x_w, y_w, z_w) = kH = k[-h + (R_1 - \sqrt{R_1^2 - x_w^2 - y_w^2}) + (R_2 - \sqrt{R_2^2 - x_w^2 - y_w^2})]. \quad (18)$$

Because the polishing spot can be seen as the round, the average pressure can be expressed by the following expression:

$$p_t = \frac{kH}{\pi(x_w^2 + y_w^2)}. \quad (19)$$

The average pressure distribution can be obtained as follows:

$$p_t(x_w, y_w, z_w) = k[-h + (R_1 - \sqrt{R_1^2 - x_w^2 - y_w^2}) + (R_2 - \sqrt{R_2^2 - x_w^2 - y_w^2})] / \pi\{[h(2R_1 - h) \times (h^2 - 2R_1h - 4R_2h + 4R_1R_2 + 4R_2^2)] / [4(R_1 + R_2 - h)^2]\}. \quad (20)$$

As  $x_w = 0, y_w = 0$ , the maximum average pressure expression on the center point in the polishing spot is

$$p_{t\max} = \frac{4k(R_1 + R_2 - h)^2}{\pi(2R_1 - h)(h^2 - 2R_1h - 4R_2h + 4R_1R_2 + 4R_2^2)}. \quad (21)$$

From Eq. (21), the maximum average on the center point of the workpiece can be obtained. According to the Preston equation  $dh/dt = K_p PV$ , the material removal rate can be expressed by the maximum depth per unit time. If the influence of the other factors on the material removal will not be considered, the maximum depth on the center point can be considered as the depth of the material removal. So, by comparing the pressure of the workpiece with the different curvature radius on the center point, the influence of the curvature radius on the material removal can be estimated.

## 2.2 Material removal considering the influence of the curvature radius in the bonnet polishing convex surface

### 2.2.1 Polishing pressure of the convex surface with different curvature radius

Fig. 2 is Local geometric model scheme of bonnet

polishing convex optical workpieces with different curvature radius.

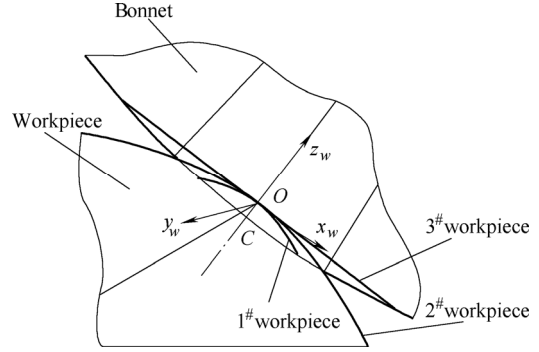


Fig. 2. Convex surface with different curvature radius

Supposing the curvature radius of the 1<sup>#</sup> is  $r_1$ , the curvature radius of the 2<sup>#</sup> is  $r_2$ , the curvature radius of the 3<sup>#</sup> is  $r_3$ , and  $r_1 < r_2 < r_3$ . Supposing the initial decrement  $OC$  is the same when the bonnet polished the workpiece by the fixed-point polishing. According to Eq. (12), the size order of contact spot is as the following:  $1^\# < 2^\# < 3^\#$ .

According to Eq. (20) of the maximum convex pressure, it can be known that the size order of the maximum pressure with the different curvature radius on the same contact point is as the following:  $3^\# < 2^\# < 1^\#$ .

### 2.2.2 Influencing of the different curvature radius on the material removal rate

The conclusion of the material removal rate can be done as the following:  $1^\# > 2^\# > 3^\#$ . The material removal rate with the smaller curvature radius on the convex workpiece is larger than that of the material removal rate with the larger curvature radius on the convex workpiece.

## 3 Influence of the Bonnet Rotational Speed on Material Removal in the Bonnet Polishing Convex Surface

If the workpiece is static ( $\omega_2 = 0$ ), the relative velocity between the bonnet and the workpiece is the line velocity at the contact point, Fig. 3 is the velocity distribution sketch of bonnet polishing convex surface.

According to Fig. 1 and from the foregoing discussion, the bonnet decrement  $h$  is very tiny compared with the bonnet curvature radius  $O_1C$ . So the point  $O$  and the point  $O'$  can be considered as the same flat, the connection line  $OO'$  is perpendicular to the line  $O_1O_2$ . The symbol  $\theta$  is the angle between  $GO$  and  $OO'$  (the axis  $x_w$  direction).

For the center point  $O$  on the polishing zone, its velocity is

$$V_o = \omega_1 \cdot |ON| = \omega_1 \cdot |OO'| \cdot \cos(\alpha). \quad (22)$$

So, the velocity vector  $G$  of any point on the contact zone can be considered as the plane during  $x$  and  $y$  coordinate system

$$V_G(x, y) = \omega_1 \cdot |O'G| \cdot \cos(\alpha), \quad (23)$$

$$|O'G| = \sqrt{|OG|^2 + |OO'|^2 - 2|OG||OO'| \cos(\pi - \theta)}. \quad (24)$$

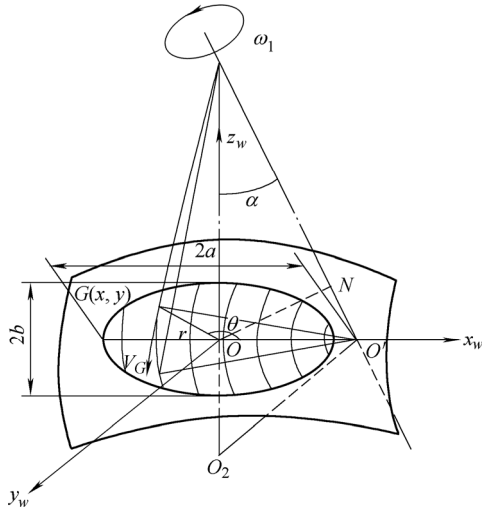


Fig. 3. Velocity distribution in the bonnet polishing convex surface

During  $x$  and  $y$  coordinate system, for any point  $G(x, y)$ , supposing  $OG = r$ ,  $OO' = (R_1 - h) \tan \alpha$ , the velocity expression of point  $G$  is

$$V_G(x, y) = \omega_1 \cos(\alpha) [(R_1 - h)^2 \tan^2(\alpha) + x^2 + y^2 + 2\sqrt{x^2 + y^2} (R_1 - h) \tan(\alpha) \cos(\theta)]^{\frac{1}{2}}. \quad (25)$$

Supposing  $r = \sqrt{x^2 + y^2}$ , the following result can be obtained according to Eq. (25):

$$V_G(r, \theta) = \omega_1 \{ [(R_1 - h) \sin(\alpha)]^2 + r^2 + r(R_1 - h) \sin(2\alpha) \cos(\theta) \}^{\frac{1}{2}}. \quad (26)$$

#### 4 Material Removal Model Considering Influence on Curvature Radius in Bonnet Polishing Convex Surface

The following conclusion can be done from the results by the author<sup>[26]</sup>: for the spherical workpieces with smaller curvature radius, the material removal rate is not proportional to the bonnet decrement. And from the above discussion in this paper, the polishing pressure on the polishing spot mainly originates from the bonnet decrement. For building the material removal model more accurately, the material removal model on the basis of the Preston equation needs to be modified according to the experimental results.

Firstly, the linear relation expression between the material removal rate and the speed on the basis of the Preston equation and the index expression between the

material removal rate and the pressure is built. Secondly, the Preston coefficient and the pressure index on the basis of the experimental results is determined. Finally the material removal model is simulated in order to determine whether the simulation results are in accordance with the actual polishing or not.

According to the foregoing analysis, the material removal model of the convex surface is

$$\frac{dH(x, y, \theta)}{dt} = k_p P^m(x, y, \theta) V(x, y, \theta), \quad (27)$$

where  $m$  is the pressure index.

Substituting Eq. (20) of the pressure distribution and substituting Eq. (25) of the velocity distribution into Eq. (27), the material removal model of the convex surface can be obtained as the following:

$$\frac{dH(x, y, \theta)}{dt} = k_p \omega_1 \times \left[ \frac{k \left[ h - (R_1 - \sqrt{R_1^2 - x^2 - y^2}) - (R_2 - \sqrt{R_2^2 - x^2 - y^2}) \right]}{\pi \frac{h(2R_1 - h)(h^2 - 2R_1h - 4R_2h + 4R_1R_2 + 4R_2^2)}{4(R_1 + R_2 - h)^2}} \right]^m \cdot \{ [(R_1 - h) \sin(\alpha)]^2 + x^2 + y^2 + \sqrt{x^2 + y^2} (R_1 - h) \sin(2\alpha) \cos(\theta) \}^{\frac{1}{2}}. \quad (28)$$

From Eq. (28), the parameters such as the bonnet curvature radius, the workpiece curvature radius, the bonnet decrement and the precession angle are considered. As  $x = 0, y = 0$ , where the material removal depth  $H_0$  is the center point  $O$ :

$$H_0 = k_p \left\{ \frac{4k(R_1 + R_2 - h)^2}{\pi(2R_1 - h)(h^2 - 2R_1h - 4R_2h + 4R_1R_2 + 4R_2^2)} \right\}^m \times (R_1 - h) \sin(\alpha) \omega_1 t. \quad (29)$$

According to Eq. (29), the center removal depth  $H_0$  can be obtained from the experiments, Preston coefficient  $k_p$  can be solved as the following:

$$k_p = \frac{H_0}{(R_1 - h) \omega_1 t \sin(\alpha)} \times \left\{ \frac{\pi(2R_1 - h)(h^2 - 2R_1h - 4R_2h + 4R_1R_2 + 4R_2^2)}{4k(R_1 + R_2 - h)^2} \right\}^m. \quad (30)$$

#### 5 Material Removal Model Verification of Convex Surface

The bonnet “precession” polishing usually is completed

by the discrete mode composed of the fixed polishing with four points in the declining manner. So the material removal in the “precession” polishing consists of the superposition of the four points polishing. Firstly the material removal model is researched and then the undermined coefficient in the model is determined. The experimental conditions of the material removal model are shown in the Table 2.

**Table 2. Experimental condition**

Parameter	Value
Curvature radius $r/\text{mm}$	50.99
Bonnet rotation speed $n/(\text{r} \cdot \text{min}^{-1})$	700
Inner pressure $p/\text{kPa}$	22
Bonnet precession angle $\alpha/(\text{°})$	25
Polishing liquid concentration $c/\%$	10
Bonnet decrement $s/\text{mm}$	0.2
Dwell time $t/\text{s}$	480

In the polishing experiments, the convex spherical workpiece with the sand optical glass surface is used, and the abrasive material is the cerium oxide polishing powder. After polishing, the Taylor Hobson was used to measure the material removal depth.

**5.1 Material removal model initialization**

Under the condition Table 2, along the radial direction of the circular polishing area, the material removal depth curve was measured as Fig. 4 and the maximum removal depth is 106.7  $\mu\text{m}$ .

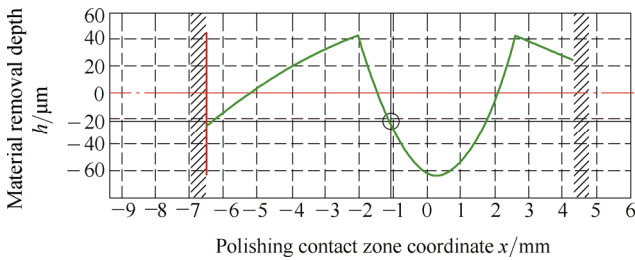


Fig. 4. Material removal depth of optical convex surface

During the material removal model derivation process, according to Eq. (28), the two coefficients are undetermined, one is Preston coefficient  $k_p$ , the coefficient  $k_p$  is related to the other process conditions except the polishing velocity and the pressure; the other is polishing pressure index  $m$ . The two coefficients all can be obtained through the experiment data. In Eq. (30), the value of the parameters  $R_1$  is set to 40 mm and the bonnet elastic coefficient  $K$  after being taken test is equal to 9.3 N/mm. The following conclusion can be done from the results by the author<sup>[26]</sup>: for the convex surface with the larger curvature radius, the material removal and the bonnet decrement can be regarded as the linear approximately. So the pressure index  $m$  is set to 1. According to Eq. (30),  $k_p$  calculation result is  $1.53 \times 10^{-13} \text{ m}^2/\text{N}$ .

**5.2 Material removal model validation**

After Preston coefficient  $k_p$  and the polishing pressure index  $m$  were solved, the material removal process can be simulated for the convex surface, the bonnet rotational speed  $n$  is set from 700 r/min to 400 r/min, and the fixed polishing experiments were done on the convex surface with the same curvature radius.

The bonnet polishing process is simulated by the MATLAB software, and the measured results are compared with the simulated results, the compared results are shown in Fig. 5.

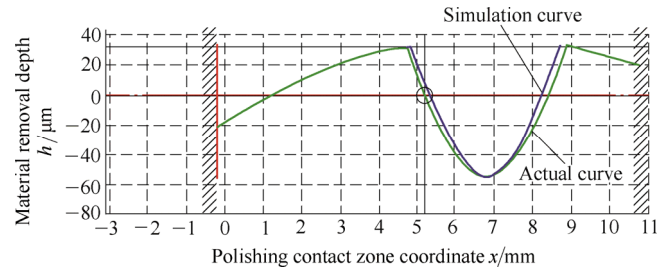


Fig. 5. Comparison between the simulation curve and the measured curve

From Fig. 5, it can be seen that the simulation curve reflects the actual material removal process. And the depth of the material removal on the simulation curve and the actual curve fits, but the size of the simulation polishing spot is smaller than that of the actual size. Because as  $m$  and  $k_p$  were being solved, the bonnet rotational speed is set to 700 r/min from 400 r/min, the actual polishing spot size changes smaller.

**5.3 Material removal model verification of the convex surface with smaller curvature radius**

The experimental conditions of the material removal model with the smaller curvature radius are shown in the Table 3.

**Table 3. Experimental condition**

Parameter	Value
Curvature radius $r/\text{mm}$	19.59
Bonnet rotation speed $n/(\text{r} \cdot \text{min}^{-1})$	300
Inner pressure $p/\text{kPa}$	23
Bonnet precession angle $\alpha/(\text{°})$	23
Polishing liquid concentration $c/\%$	10
Bonnet decrement $s/\text{mm}$	0.2
Dwell time $t/\text{s}$	480

Under the condition Table 3, along the radial direction of the circle polishing spot, the material removal depth measured is about 109  $\mu\text{m}$ . Firstly, according to the research, the polishing pressure index  $m$  is determined. The figure after fitting is shown as Fig. 6. From Fig. 6, according to the curve figure after fitting, the equation  $m = 2/5$  can be obtained. According to Eq. (29), the coefficient of Preston equation  $k_p = 7.12 \times 10^{-13}$  is calculated, the bonnet rotational speed is set from 300

r/min to 800 r/min.

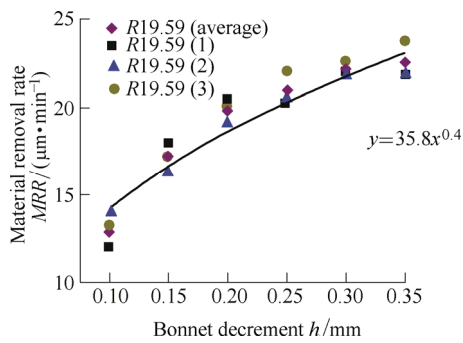


Fig. 6. Determination pressure factor in bonnet polishing

The fixed polishing experiments are done on the convex surface with the same curvature radius, and at the same time the other parameters remain unchanged, the results from these experiments are compared, the compared figure is shown as Fig. 7.

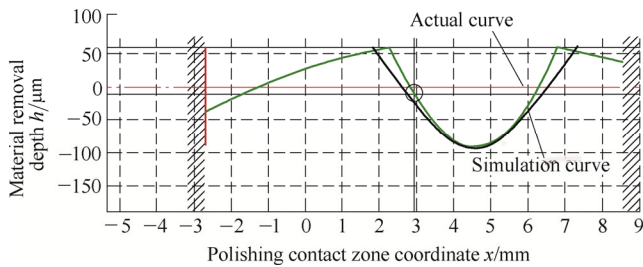


Fig. 7. Comparison between simulated curve and measured curve

From Fig. 7, it can be seen that the depth of material removal between the simulated curve and the measured curve fits, the simulation reflects the actual material removal process.

## 6 Conclusions

The prediction of the material removal can help to realize the automatic control. The research on the material removal model is the basis of the material removal mechanical automation. For the convex surface, the paper has been presented four innovations.

(1) The calculation expression of the polishing contact spot on the convex surface considering the curvature radius has been deduced;

(2) The calculation expression of the pressure distribution which relates with the bonnet curvature radius and the workpiece curvature radius has been deduced;

(3) The calculation expression of the velocity on the convex surface has been deduced;

(4) By the combination method of the theoretical expression derivation and the experimental verification, the semi-empirical material removal model has been built and the material removal model correctness has been verified.

## References

- [1] WALKER D D, BEAUCAMP A T H, BINGHAM R G, et al. Precessions process for efficient production of aspheric optics for large telescope and their instrumentation[J]. *Proc. SPIE*, 2003, 4842: 73–84.
- [2] WALKER D D, BEAUCAMP A T H, BROOKS D, et al. Novel CNC polishing process for control of form and texture on aspheric surfaces[J]. *Proc. SPIE*, 2002, 4767: 99–106.
- [3] WALKER D D, BEAUCAMP A T H, BROOKS D, et al. New results from the precession polishing process scaled to larger sizes[J]. *Proc. SPIE*, 2004, 5494: 71–81.
- [4] WALKER D D, KIM S W, BINGHAM R G, et al. Computer-controlled polishing of moderate-sized general aspherics for instrumentation[J]. *Proc. SPIE*, 1998, 3355: 947–954.
- [5] BINGHAM R G, WALKER D D, KIM D H, et al. Novel automated process for aspheric surfaces[J]. *Proc. SPIE*, 2004, 4093: 445–450.
- [6] WALKER D D, BEAUCAMP A T H, BINGHAM R G, et al. Precessions aspheric polishing: new results from the development program[J]. *Proceeding of SPIE-The International Society for Optical Engineering*, 2003, 5180: 15–28.
- [7] JACOBS S D. International innovations in optical finishing[J]. *Proceedings of The Society of Photo-Optical Instrumentation Engineers (SPIE)*, 2004, 5523: 264–272.
- [8] KIM D W, KIM S W. Novel simulation technique for efficient fabrication of 2-m class hexagonal segments for extremely large telescope primary mirrors[J]. *Proc. SPIE*, 2005, 5638: 48–59.
- [9] KIM D W, KIM S W. Static tool influence function for fabrication simulation of hexagonal mirror segments for extremely large telescopes[J]. *Optics Express*, 2005, 13: 910–917.
- [10] BEAUCAMP A, NAMBA Y, CHARLTON P. Corrective finishing of extreme ultraviolet photomask blanks by precessed bonnet polisher[J]. *Applied Optics*, 2014, 53(14): 3075–3080.
- [11] BEAUCAMP A, NAMBA Y, INASAKI I, et al. Finishing of optical moulds to  $\lambda/20$  by automated corrective polishing[J]. *CRIP Annal-Manufacturing Technology*, 2011(60): 375–378.
- [12] PAN Ri, WANG Zhenzhong, WANG Chunjin, et al. Research on the precession motion control technology for free surface optical elements in bonnet polishing[J]. *Journal of Mechanical Engineering*, 2013, 49(3): 186–193. (in Chinese)
- [13] PAN Ri, YANG Wei, WANG Zhenzhong, et al. The controllable bonnet polishing system for large diameter aspheric optical elements in bonnet polishing[J]. *Laser and Particle Beams*, 2012, 24(6): 1344–1348.
- [14] WANG Chunjin, YANG Wei, WANG Zhenzhong, et al. Dwell-time algorithm for polishing large optics[J]. *Applied Optics*, 2014, 53(21): 4752–4760.
- [15] WANG C, WANG Z, YANG X, et al. Modeling of the static tool influence function of bonnet polishing based on FEA[J]. *International Journal of Advanced Manufacturing Technology*, 2014, 74(1–4): 341–349.
- [16] WANG Chunjin, YANG Wei, YE Shiwei, et al. Optimization of parameters for bonnet polishing based on the minimum residual error method[J]. *Optical Engineering*, 2014, 53(7): 075108(1–9).
- [17] JI S M, ZHANG L, ZHANG X, et al. Spinning-inflated-ballonet polishing tool and its application in curved surface polishing[J]. *Key Engineering Materials*, 2007, 339: 21–25.
- [18] JI S M, ZHANG X, ZHANG L, et al. Form and texture control of free-form surface polishing[J]. *Key Engineering Materials*, 2006, 304–305: 113–117.
- [19] JI Shiming, YUAN Qiaoling, ZHANG Li, et al. Study of the removing depth of the polishing surface based on a novel spinning-inflated-ballonet polishing tool[J]. *Materials Science Forum*, 2006, 532–533: 452–455.
- [20] JIN Mingsheng, JI Shiming, ZHANG Li, et al. The optimization of the line space and experimental research on the continuous precession in bonnet polishing[J]. *China Mechanical Engineering*,

- 2013, 24(7): 861–865.
- [21] ZHANG Li, LI Yanbiao, JIN Mingsheng, et al. Analysis of the abrasive field to polish mold free surface in new bonnet polishing[J]. *China Mechanical Engineering*, 2014, 25(6): 832–835.
- [22] CONG Kai. *3-PRS CNC system development of bonnet polishing parallel machine*[D]. Harbin: Harbin Institute Technology, 2010.
- [23] XIE Dagang, GAO Bo, YAO Yingxue, et al. Study of local material removal model of bonnet tool polishing[J]. *Key Engineering Materials*, 2006, 304–305: 335–339.
- [24] PRESTON F W. The theory and design of plate glass polishing[J]. *Journal of the Society of Glass Technology*, 1927, 11: 214–256.
- [25] JOHNSON K L. *Contact mechanics*[M]. Beijing: High Education Press, 1992.
- [26] SONG Jianfeng, YAO Yingxue, XIE Dagang, et al. Effects of

polishing parameters on material removal for curved optical glasses in bonnet polishing[J]. *Chinese Journal of Mechanical Engineering*, 2008, 21(5): 29–33.

### Biographical notes

SONG Jianfeng is currently associate professor at *College of Mechanical Engineering, Yanshan University, China*. She graduated from *Harbin Institute Technology, China*, in October, 2009. Her research interests include intelligent manufacturing and digital manufacturing.

E-mail: songjianfeng@ysu.edu.cn

YAO Yingxue is currently a professor at *School of Mechatronics Engineering, Harbin Institute Technology, China*.